J Solid State Electrochem (2003) 7: 113–117
DOI 10.1007/s10008-002-0314-3

ORIGINAL PAPER

**Antonija Dindune · Zaiga Kanepe**
**Edvardas Kazakevičius · Algimantas Kežionis**
**Janis Ronis · Antanas Feliksas Orliukas**

# Synthesis and electrical properties of $Li_{1+x}M_xTi_{2-x}(PO_4)_3$ (where $M$ = Sc, Al, Fe, Y; $x$ = 0.3) superionic ceramics

Received: 26 September 2001 / Accepted: 22 December 2001 / Published online: 27 September 2002
© Springer-Verlag 2002

**Abstract** Compounds of the system $Li_{1+x}M_xTi_{2-x}(PO_4)_3$ (where $M$ = Sc, Al, Fe, Y; $x$ = 0.3) were synthesized by a solid-state reaction and studied by X-ray diffraction. The ceramic samples were sintered and investigated by complex impedance spectroscopy in the frequency range $10^6$–$1.2\times10^9$ Hz in the temperature range 300–600 K. Two relaxation dispersions related to the fast $Li^+$ ion transport in bulk and grain boundaries were found. The activation energies of the bulk conductivity and relaxation frequency were obtained from the slops of Arrhenius plots. The values of the activation energies of the bulk ionic conductivity and relaxation frequency were found to be very similar in all the materials investigated. That can be attributed to the fact that the temperature dependences of the bulk conductivity are caused only by the mobility of the fast $Li^+$ ions, while the number of charge carriers remains constant with temperature.

**Keywords** Solid electrolyte ceramics · Fast ion transport · Ionic conductivity

## Introduction

Lithium ion conductors with high conductivity are especially attractive materials for development of rechargeable batteries [1] and $CO_2$ gas sensors [2]. It has already been reported [3] that the conductivity of $LiTi_2(PO_4)_3$ increases noticeably if the $Ti^{4+}$ cation is partially substituted by a cation such as $M^{3+}=Sc^{3+}$, $Al^{3+}$, $Y^{3+}$, $Fe^{3+}$ or $La^{3+}$. So-synthesized compounds of the $Li_{1+x}M_xTi_{2-x}(PO_4)_3$ system are known as low-temperature solid electrolytes with fast $Li^+$ ion transport [3, 4]. The values of the ionic conductivity, their activation energy and the lattice constants of the compounds of this system depend on the ionic radius of the substituting metal and on the $x$ value (the compounds with $M_x=Sc_{0.3}$, $Al_{0.3}$ or $Fe_{0.3}$ belong to the rhombohedral symmetry space group $R\bar{3}c$ [3, 4, 5, 6]).

The substitution $Ti^{4+}\rightarrow Y^{3+}(La^{3+})+Li^+$ in $LiTi_2(PO_4)_3$ causes the formation of a solid solution of the mixed $LiTi_2(PO_4)_3$ and $Li_3Y_2(La_2)(PO_4)_3$ phases [4]. At 298 K in a low-frequency electric field ($v=10^3$ Hz) the values of the total conductivity of the compounds with $M_x=Sc_{0.3}$, $Al_{0.3}$, $Fe_{0.3}$ or $Y_{0.4}$ or $La_{0.3}$ were found to be $4\times10^{-2}$, $7\times10^{-2}$, $2.5\times10^{-2}$, $6\times10^{-4}$ and $5\times10^{-4}$ $Sm^{-1}$, respectively [3, 7]. Their good chemical stability in air and high ionic conductivity at room temperature stimulate further investigations of these materials. The present work continues our studies [8, 9, 10] on $Li^+$ conductive ceramics based on $LiTi_2(PO_4)_3$ with the partial substitution by Sc, Al, Fe or Y. We report the synthesis conditions of powders of $Li_{1+x}M_xTi_{2-x}(PO_4)_3$ (where $M_x=Sc_{0.3}$, $Al_{0.3}$, $Fe_{0.3}$, $Y_{0.3}$), sintering of the ceramic samples, the results of our X-ray investigations, the bulk, $\sigma_b$, the grain boundary, $\sigma_{gb}$, and the total, $\sigma_{tot}$, conductivity of the ceramic materials at frequencies from $10^6$ to $1.2\times10^9$ Hz in the temperature range 300–600 K.

Presented at the Regional Seminar on Solid-State Ionics, Jūrmala, Latvia, 22–26 September 2001

A. Dindune · Z. Kanepe · J. Ronis
Institute of Inorganic Chemistry,
Riga Technical University,
Miera iela 34, 2169 Salaspils, Latvia

E. Kazakevičius (✉) · A. Kežionis · A.F. Orliukas
Department of Physics,
Vilnius University, Saulėtekio al. 9,
2040 Vilnius, Lithuania
E-mail: edvardas.kazakevicius@ff.vu.lt
Tel.: +370-2-366064
Fax: +370-2-366081

## Experimental

Powder of the compounds of the $Li_{1+x}M_xTi_{2-x}(PO_4)_3$ systems (where $M_x=Sc_{0.3}$, $Al_{0.3}$, $Fe_{0.3}$, $Y_{0.3}$) were synthesized from a stoichiometric mixtures of $Li_2CO_3$ (purity 99.999%), extra pure $NH_4H_2PO_4$, $M_2O_3$ (where $M$ = Sc, Al, Fe, Y) and $TiO_2$ by a solid-phase reaction. Each mixture was milled for 8 h in an agate mill in

ethyl alcohol. After milling, the synthesis of powders with $M_x$= $Al_{0.3}$, $Fe_{0.3}$ or $Y_{0.3}$ followed this sequence: heating of the mixtures at 723 K (for Al, Fe) and at 773 K (for Y) for 24 h, milling for 12 h, heating of the powder at 1,173 K for 1 h and at 1,273 K for 2 h. After cooling to room temperature, the powder was placed in ethyl alcohol and milled in a planetary mill for 8 h. The fine powder was dried at 393 K for 24 h. The synthesis of the $Li_{1.3}Sc_{0.3}Ti_{1.7}(PO_4)_3$ powder was slightly different: heating at 423 K for 20 h, milling for 10 h, heating at 723 K for 24 h, milling for 8 h, heating three times to 1,153 K and milling for 10 h. A planetary mill was also used for milling the emulsions of the powders with ethyl alcohol. The particle size of the dried powder was found to be 5 μm on average for compounds with $M$ = Al, Fe or Y and about 1 μm for the compound with M = Sc. The powders obtained were uniaxially cold-pressed into pellets at a pressure of 300 MPa. The sintering temperatures of the ceramic samples of the systems with $M_x$ = $Sc_{0.3}$, $Al_{0.3}$, $Fe_{0.3}$ or $Y_{0.3}$ were 1,543, 1,383, 1,283 and 1,293 K respectively. The samples of each compound were sintered in air for 1 h. The structural parameters of all the powders were obtained from the X-ray diffraction patterns using Cu $K_{\alpha 1}$ radiation. The patterns were step-scanned [1° ($2\theta$)/60 s] in the region of $2\theta$ = (6–80)°. The measurements of the electric properties were conducted in air using a coaxial impedance spectrometer setup [10]. A part of a coaxial line was used as a sample holder. The ceramic sample was placed between two pieces of inner conductor of the line and transmittance coefficient, $T_x$, of this section of the line was measured at different frequencies and temperatures. Pellets of 3.5 mm diameter and 1.5 mm thickness were used for our measurements. The complex impedance, $Z_x$, of the sample in its holder may be expressed as

$$\frac{1}{Z_x} = i\omega\left[A_2\left(C_p + C_1\right) - C_p + C_0\right], \quad (1)$$

where $\omega = 2\pi v$ is the angular frequency of the electrical field, $C_0$ is the geometrical capacitance of a sample with dielectric permittivity $\epsilon = 1$, i.e. $C_0 = \epsilon_0 S/d$, where $S$ and $d$ are the area and the thickness of the sample under investigation and $\epsilon_0$ is the dielectric constant of a vacuum($8.85\times10^{-12}$ $Fm^{-1}$), $C_p = (A_1C_1 - C_2)/(1 - A_1)$ is a parasitic capacity, and $C_1$ and $C_2$ are the capacities of two calibration samples. $A_1$ and $A_2$ are

$$A_1 = \frac{T_0/T_1 - 1}{T_0/T_2 - 1}, \quad A_2 = \frac{T_0/T_1 - 1}{T_0/T_x - 1}, \quad (2)$$

where $T_0$, $T_1$ and $T_2$ are calibration transmittance coefficients for the cases when the sample holder in the central line is shortened and calibration samples of capacity $C_1$ and $C_2$ are inserted, respectively, and $T_x$ is the transmittance coefficient in the system with the sample investigated.

In the frequency range from $10^6$ to $1.25\times10^9$ Hz, the calibration and measurements were performed by means of a computerized system for a set of 64 fixed frequencies. Primary processing of the data and the plotting of the frequency dependence of the impedance, admittance, dielectric permittivity and electric modulus were performed and controlled in real time. The temperature was measured using a K-type thermocouple. The thermocouple was placed near the sample. The measurements can be carried out in the temperature region from 300 to 1,200 K. The error of the temperature measurements in the temperature range investigated did not exceed ±1 K.

## Results and discussion

The results of the X-ray investigations have shown that the compounds, obtained by the substitution $Ti^{4+} \rightarrow Sc^{3+}$, $(Al^{3+})$, $(Fe^{3+}) + Li^+$ in the $Li_{1+x}M_xTi_{2-x}(PO_4)_3$ (where $x = 0.3$) system are single-phase materials (Table 1). A small amount of $YPO_4$ was detected in $Li_{1.3}Y_{0.3}Ti_{1.7}(PO_4)_3$ as an impurity. The results revealed changes in the interplanar distances with the change of substituting atoms in the superionic material. The lattice parameters, unit cell volume and density of the materials are presented in Table 2. All four compounds have rhombohedral symmetry (space group $R\bar{3}c$) with six formula units in a unit cell. The density of the ceramic samples was found to be on average 88–93% of the value of the theoretical density.

Complex impedance spectroscopy at alternating electric fields of variable frequency has been extensively used to distinguish between different mechanisms contributing to the charge transport [12, 13, 14]. High-frequency impedance measurements of ionic conductors allow elimination of the effects caused by the blocking processes between electrodes and the superionic material and also separating charge transport processes in a grain and grain boundary of ceramics at high temperature. The impedance spectra of superionic materials consist of two overlapped dispersion regions: the high-frequency part may be attributed to the relaxation in bulk, while the lower part corresponds to grain boundary processes as in a wide range of other ceramic conducting materials [15, 16, 17]. Owing to the apparent thermally activated nature, both processes, bulk and grain boundary relaxations, shift toward the high-frequency range with an increase in the temperature. The observed relaxation-type dispersions can be analyzed using the frequency dependences of the impedance in the complex plane. It is a representation of the complex impedance ($\dot{Z} = Z' + Z''$) as a $Z''$ ($Z'$) dependence. Examples of the complex impedance plots of the $Li_{1.3}Y_{0.3}Ti_{1.7}(PO_4)_3$ ceramic sample at 300, 455 and 575 K are shown in Fig. 1. The plots consist of two overlapped semicircles with centers below the real axis. The relaxation process in the bulk causes the high-frequency arc, and the low-frequency arc is related to the relaxation process in the intragrain areas of the ceramic samples. The frequencies of the relaxation dispersion shift with temperature into the higher-frequency region and, when $T > 500$ K, a relaxation process in the bulk occurs outside the frequency region investigated by us. At high temperature, when the conductivity increases, deviation from the symmetrical low-frequency semicircle appears on the right shoulder owing to blocking Pt contacts of a sample (Fig. 1c). For the quantitative analysis of the spectra a simplified equivalent circuit of two resistors in series, each shunted by a constant phase element [18], was used. Such a circuit can be described by the sum of two Cole–Cole expressions [19, 20], which represent depressed semicircles with centers below the real axis. The temperature dependence of the bulk ionic conductivity, $\sigma_b = Z_b^{-1}$ (where $Z_b$ is the impedance of bulk) is shown in Fig. 2. The activation energy of the bulk conductivity, $\Delta E_b$, is calculated according to the Arrhenius equation:

$$\sigma_b = \frac{\sigma_0}{T}\exp\left(-\frac{\Delta E_b}{kT}\right), \quad (3)$$

where $k = 1.38\times10^{-23}$ $JK^{-1}$ is the Boltzmann constant. This equation is widely used to parameterize measured

**Table 1** X-ray powder diffraction results for $LiTi_2(PO_4)_3$ [11], $Li_{1.3}Sc_{0.3}Ti_{1.7}(PO_4)_3$, $Li_{1.3}Al_{0.3}Ti_{1.7}(PO_4)_3$, $Li_{1.3}Fe_{0.3}Ti_{1.7}(PO_4)_3$ and $Li_{1.3}Y_{0.3}Ti_{1.7}(PO_4)_3$

| $LiTi_2(PO_4)_3$ | | $Li_{1.3}Sc_{0.3}Ti_{1.7}(PO_4)_3$ | | $Li_{1.3}Al_{0.3}Ti_{1.7}(PO_4)_3$ | | $Li_{1.3}Fe_{0.3}Ti_{1.7}(PO_4)_3$ | | $Li_{1.3}Y_{0.3}Ti_{1.7}(PO_4)_3$ | |
|---|---|---|---|---|---|---|---|---|---|
| $d$ (Å) | $I/I_0$, (%) | $d$ (Å) | $I/I_0$, (%) | $d$ (Å) | $I/I_0$, (%) | $d$ (Å) | $I/I_0$, (%) | $d$ (Å) | $I/I_0$, (%) |
| 6.017 | 13 | 6.07 | 15 | 6.03 | 23 | 5.99 | 29 | 6.01 | 23 |
| 4.258 | 80 | 4.27 | 57 | 4.73 | 3 | 5.04 | 5 | 4.25 | 60 |
| 3.632 | 100 | 3.65 | 100 | 4.27 | 68 | 4.25 | 62 | 3.63 | 100 |
| 3.477 | 8 | 3.490 | 7 | 4.09 | 9 | 4.02 | 2 | 3.473 | 7 |
| 3.011 | 28 | 3.022 | 30 | 3.636 | 100 | 3.951 | 2 | 3.002 | 30 |
| 2.761 | 20 | 2.772 | 15 | 3.480 | 8 | 3.754 | 2 | 2.758 | 14 |
| 2.694 | 26 | 2.705 | 22 | 3.255 | 10 | 3.619 | 100 | 2.689 | 24 |
| 2.457 | 25 | 2.467 | 19 | 3.016 | 26 | 3.466 | 7 | 2.456 | 17 |
| 2.3180 | 1 | 2.134 | 3 | 2.7615 | 17 | 3.243 | 3 | 2.128 | 5 |
| 2.1291 | 3 | 2.042 | 9 | 2.6921 | 23 | 2.998 | 31 | 2.033 | 8 |
| 2.0351 | 12 | 2.014 | 3 | 2.4947 | 3 | 2.755 | 15 | 2.005 | 3 |
| 2.0065 | 2 | 1.9102 | 13 | 2.4577 | 17 | 2.683 | 23 | 1.9019 | 14 |
| 1.9043 | 17 | 1.8412 | 3 | 2.1910 | 2 | 2.455 | 16 | 1.8346 | 5 |
| 1.8360 | 5 | 1.8205 | 12 | 2.1318 | 2 | 2.122 | 3 | 1.8138 | 14 |
| 1.8147 | 16 | 1.7446 | 2 | 2.0359 | 9 | 2.032 | 8 | 1.7357 | 2 |
| 1.7397 | 2 | 1.6900 | 5 | 2.0060 | 2 | 1.9027 | 15 | 1.6848 | 5 |
| 1.6862 | 6 | 1.6754 | 6 | 1.9028 | 14 | 1.8343 | 3 | 1.6681 | 5 |
| 1.6706 | 7 | 1.6137 | 15 | 1.8365 | 2 | 1.8139 | 11 | 1.6073 | 15 |
| 1.6087 | 22 | 1.5725 | 4 | 1.8160 | 12 | 1.6807 | 5 | 1.5659 | 5 |
| 1.5674 | 7 | 1.5094 | 2 | 1.7411 | 2 | 1.6667 | 7 | 1.5036 | 2 |
| 1.5052 | 3 | 1.4744 | 1 | 1.6865 | 5 | 1.6078 | 15 | 1.4696 | 6 |
| 1.4710 | 2 | 1.4648 | 7 | 1.6695 | 5 | 1.5679 | 5 | 1.4582 | 3 |
| 1.4602 | 8 | 1.4229 | 4 | 1.6104 | 16 | 1.4588 | 8 | 1.4177 | 4 |
| 1.4188 | 5 | 1.3941 | 2 | 1.5694 | 5 | 1.4192 | 3 | 1.3891 | 5 |
| 1.3900 | 3 | 1.3859 | 3 | 1.5055 | 2 | 1.3803 | 3 | 1.3796 | 3 |
| | | 1.3505 | 3 | 1.4609 | 7 | 1.3456 | 2 | 1.3449 | 5 |
| | | 1.3253 | 4 | 1.4200 | 5 | 1.3210 | 5 | 1.3205 | 4 |
| | | 1.3175 | 2 | 1.3912 | 2 | | | 1.3123 | 2 |
| | | 1.2869 | 3 | 1.3822 | 3 | | | 1.2827 | 3 |
| | | | | 1.3467 | 3 | | | | |
| | | | | 1.3220 | 5 | | | | |
| | | | | 1.3141 | 3 | | | | |

**Table 2** Lattice constants, unit cell volume and density of the compounds of $Li_{1+x}M_xTi_{2-x}(PO_4)_3$

| Compound | Lattice constants (Å) | | Unit cell volume (Å$^3$) | Density, (gcm$^{-3}$) |
|---|---|---|---|---|
| | $a$ | $c$ | | |
| $Li_{1.3}Sc_{0.3}Ti_{1.7}(PO_4)_3$ | 8.5354(12) | 20.9339(52) | 1,320.77 | 2.930 |
| $Li_{1.3}Al_{0.3}Ti_{1.7}(PO_4)_3$ | 8.5049(6) | 20.820(3) | 1,304.3 | 2.928 |
| $Li_{1.3}Fe_{0.3}Ti_{1.7}(PO_4)_3$ | 8.5109(10) | 20.870(2) | 1,309.2 | 2.983 |
| $Li_{1.3}Y_{0.3}Ti_{1.7}(PO_4)_3$ | 8.5087(7) | 20.830(3) | 1,306.0 | 3.066 |

conductivity data. The preexponential factor is inversely proportional to temperature, which is why we present the bulk conductivity as $\sigma_b T$ in Fig. 2.

The temperature dependences of the total conductivity, $\sigma_{tot}$, of the ceramic samples investigated are shown in Fig. 3. The activation energy of $\sigma_{tot}$ (marked as $\Delta E_{tot}$) is also calculated according to the Arrhenius equation. The results of the measurements of $\sigma_b$, $\sigma_{tot}$, $\Delta E_b$ and $\Delta E_{tot}$ of the ceramic samples are presented in Table 3.

The relaxation frequency, $f_b$, of the relaxation process in the bulk of the ceramic samples was obtained from the maximum of the frequency dependence of $Z''$ at different temperatures. The relaxation frequencies of the dispersion of $\sigma_b$ are shown as a function of temperature in Fig. 4. The relaxation frequencies in the bulk of the ceramic samples increase with temperature according to the formula

$$f_b = f_0 \exp\left(-\frac{\Delta E_f}{kT}\right), \tag{4}$$

where $f_0$ is a frequency related to the lattice vibrations and $\Delta E_f$ is the activation energy of $f_b$. The values of $f_b$ at 300 K and their activation energies for all the materials investigated are presented in Table 4.

The comparison of the estimated values of $\Delta E_b$ and $\Delta E_f$ shows that for the same compound these energies are approximately equal. The ionic conductivity of the bulk is the product of the volume concentration, $n$, of mobile $Li^+$ ions, their electric mobility, μ, and the electric charge, $q$:

$$\sigma = \mu n q, \tag{5}$$

where $q = ze$, where $z$ is the valence of the charged $Li^+$ ions ($z = 1$) and $e$ is the electron charge. The charge carrier concentration and the mobility can be thermally activated if an association of charge carriers in defect

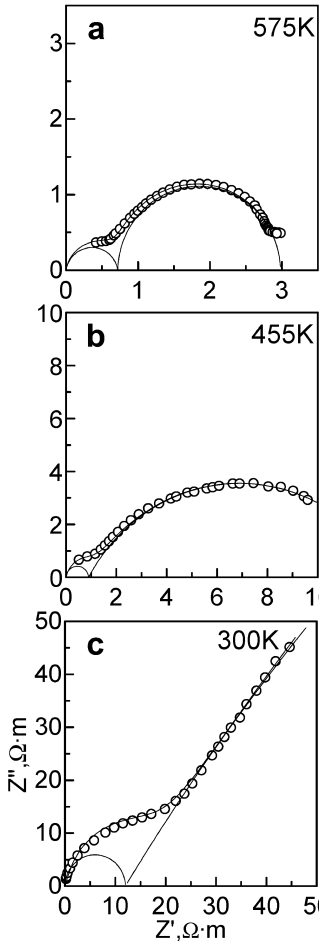


**Fig. 1a–c** Complex plane impedance plots of a $Li_{1.3}Y_{0.3}Ti_{1.7}(PO_4)_3$ ceramic sample at different temperatures

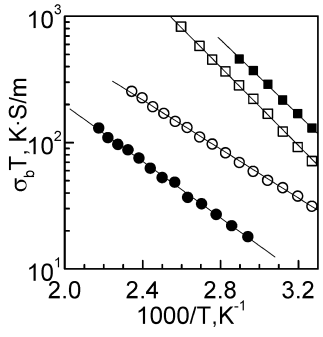


**Fig. 2** Temperature dependences of the bulk conductivity of ceramic samples of $Li_{1+x}M_xTi_{2-x}(PO_4)_3$, where $M_x = Sc_{0.3}$ (*closed circles*), $M_x = Y_{0.3}$ (*open circles*), $M_x = Al_{0.3}$ (*closed squares*) and $M_x = Fe_{0.3}$ (*open squares*)

complexes occurs [21, 22]. The temperature dependence of the ionic conductivity can be expressed as

$$\sigma = \left[n_0 \exp\left(-\frac{\Delta E_N}{kT}\right)\right]\left[\frac{C}{kT}\exp\left(-\frac{\Delta E_\mu}{kT}\right)\right]q, \qquad (6)$$

where $\Delta E_N$ is the activation energy of the mobile carrier

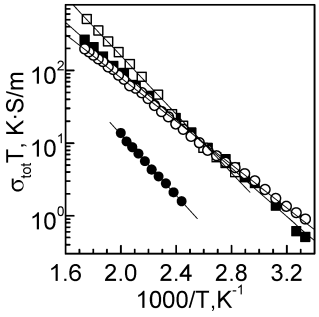


**Fig. 3** Temperature dependences of the total conductivity of ceramic samples of $Li_{1+x}M_xTi_{2-x}(PO_4)_3$, where $M_x = Sc_{0.3}$ (*closed circles*), $M_x = Y_{0.3}$ (*open circles*), $M_x = Al_{0.3}$ (*closed squares*) and $M_x = Fe_{0.3}$ (*open squares*)

**Table 3** The values of $\sigma_b$, $\sigma_{tot}$, $\Delta E_b$ and $\Delta E_{tot}$ of the compounds of $Li_{1+x}M_xTi_{2-x}(PO_4)_3$

| Composition | $\sigma_{tot}$ at 450 K ($Sm^{-1}$) | $\Delta E_{tot}$ (eV) | $\sigma_b$ at 300 K ($Sm^{-1}$) | $\Delta E_b$ (eV) |
|---|---|---|---|---|
| $Li_{1.3}Sc_{0.3}Ti_{1.7}(PO_4)_3$ | $9.6\times10^{-3}$ | 0.42 | $2.1\times10^{-2}$ | 0.20 |
| $Li_{1.3}Al_{0.3}Ti_{1.7}(PO_4)_3$ | $9.0\times10^{-2}$ | 0.33 | $3.5\times10^{-1}$ | 0.30 |
| $Li_{1.3}Fe_{0.3}Ti_{1.7}(PO_4)_3$ | $1.2\times10^{-1}$ | 0.40 | $2.2\times10^{-1}$ | 0.31 |
| $Li_{1.3}Y_{0.3}Ti_{1.7}(PO_4)_3$ | $8.0\times10^{-2}$ | 0.30 | $9.4\times10^{-2}$ | 0.19 |

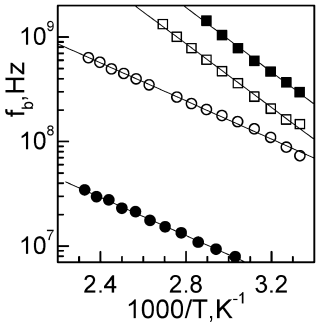


**Fig. 4** Temperature dependences of frequencies of the relaxation processes in the bulk of ceramic samples of $Li_{1+x}M_xTi_{2-x}(PO_4)_3$, where $M_x = Sc_{0.3}$ (*closed circles*), $M_x = Y_{0.3}$ (*open circles*), $M_x = Al_{0.3}$ (*closed squares*) and $M_x = Fe_{0.3}$ (*open squares*)

**Table 4** Values of $f_b$ and $\Delta E_f$ of the $Li_{1+x}M_xTi_{2-x}(PO_4)_3$ compounds at temperature 300 K

| Compound | $f_b$ (Hz) | $\Delta E_f$ (eV) |
|---|---|---|
| $Li_{1.3}Sc_{0.3}Ti_{1.7}(PO_4)_3$ | $4.0\times10^6$ | 0.19 |
| $Li_{1.3}Al_{0.3}Ti_{1.7}(PO_4)_3$ | $3.0\times10^8$ | 0.30 |
| $Li_{1.3}Fe_{0.3}Ti_{1.7}(PO_4)_3$ | $1.3\times10^8$ | 0.30 |
| $Li_{1.3}Y_{0.3}Ti_{1.7}(PO_4)_3$ | $7.3\times10^7$ | 0.19 |

formation, $n_0$ is the maximum possible concentration of charge carriers, $\Delta E_\mu$ is the activation energy for their migration and $C$ is a constant [23]. The activation energy of $\sigma_b$ is the sum $\Delta E_b = \Delta E_N + \Delta E_\mu$. From the conductivity measurement alone it is therefore not possible to separate the contributions of mobile carrier formation and their mobility from $\sigma_b$. According to the Nernst–Einstein relation, $\mu$ and the diffusion coefficient, $D$, of the mobile ions are directly proportional:

$$\mu = qD/kT. \tag{7}$$

The values of the activation energies of $D$ and $\mu$ are equal. According to the random-walk model of thermally activated jumps, the diffusion coefficient of mobile ions is related to the mean jump frequency, $\omega$, by the expression

$$D = \chi\gamma l^2\omega, \tag{8}$$

where $\omega = 2\pi f_b$, $\chi = 1/4$ is the geometric factor for a two-dimensional conductivity path in the rhombohedral site symmetry, $l^2$ is the mean-square jump distance between the cation sites in the crystal lattice and $\gamma$ is the correlation factor. Since we have found that for the same material the activation energy of $\sigma_b$ is equal to the activation energy of $f_b$, which may be attributed to the migration of $Li^+$ ion, from Eqs. (6) and (7) it follows that the concentration of charge carriers remains constant with temperature for the temperatures investigated. Such ion transport peculiarities are characteristic for oxygen [23, 24] and $Na^+$ solid electrolytes [15].

## Conclusions

Solid electrolyte compounds of $Li_{1+x}M_xTi_{2-x}(PO_4)_3$ (where $M_x = Sc_{0.3}$, $Al_{0.3}$, $Fe_{0.3}$, $Y_{0.3}$) were synthesized by solid-phase reactions and studied by X-ray diffraction and complex impedance spectroscopy in the frequency range from $10^6$ to $1.2\times10^9$ Hz in the temperature range from 300 to 600 K. Two regions of the impedance dispersion were analyzed in terms of the fast $Li^+$ ion transport in the grain boundaries and the bulk of the ceramic samples. The temperature dependences of the bulk conductivity and relaxation frequency in the bulk are governed by the same activation energy. This suggests that fast $Li^+$ ion transport in the bulk of the investigated compounds may be described mainly by the temperature-dependent mobility, while the concentration of mobile ions remains constant with temperature.

**Acknowledgement** This work was supported by the Lithuanian State Science and Education Foundation under grant "Sensors".

## References

1. Broussely M, Planchat JP, Rigobert G, Virey D, Sarre G (1997) J Power Sources 68:8
2. Salam F, Weppner W (1999) Ionics 5:355
3. Subramanian MA, Subramanian R, Clearfield A (1986) Solid State Ionics 18–19:562
4. Aono H, Sugimoto E, Sadaoka Y, Imanaka N, Adachi G (1990) J Electrochem Soc 137:1023
5. Clearfield A, Subramanian MA, Subramanian R (1985) Lithium: current applications in science, medicine and technology. Wiley, New York
6. Lin Z-X, Yu H-J, Li S-C, Tian S-B (1988) Solid State Ionics 31:91
7. Adachi G, Imanaka N, Aono H, Sugimoto E, Sadaoka Y, Yasuda N, Hara T, Nagata M (1991) US Patent 4,985,317 (Jan 15)
8. Kežionis A, Orliukas A, Dindune A, Kanepe Z (1998) Lithuanian J Phys 38:298
9. Dindune A, Kežionis A, Kanepe Z, Kazakevičius E, Sobiestianskas R, Orliukas A (1999) J Inorg Phosph Chem Phosphorus Res Bul 10:387
10. Sobiestianskas R, Dindune A, Kanepe Z, Ronis J, Kezionis A, Kazakevicius A, Orliukas A (2000) Mater Sci Eng B 76:184
11. ASTM X-ray powder diffraction file inorganic. USA, Philadelphia (1978), No 35–754
12. Bauerle JE (1969) J Phys Chem Solids 30:2657
13. Macdonald JR (1974) J Chem Phys 61:3977
14. Boukamp BA (1986) Solid State Ionics 20:31
15. Bogusz W, Dygas JR, Krok F, Kezionis A, Sobiestianskas R, Kazakevicius E, Orliukas A (2001) Phys Status Solidi A 183:323
16. Godickemeier M, Michel B, Orliukas A, Bohac P, Sasaki K, Gauckler L (1994) J Mater Res 9:1228
17. Jakubowski W, Whitmore J (1979) J Am Ceram Soc 62:381
18. Macdonald JR (1985) J Appl Phys 58:1971
19. Macdonald JR (1984) Solid State Ionics 13:147
20. Dygas JR (1986) PhD thesis. Northwestern University, Ill
21. Badwal SPS (1984) J Mater Sci 19:1767
22. Nowick AS, Park DS (1976) In: Mahan G, Roth W (eds) Superionic conductors. Plenum, New York, p 395
23. Orliukas A, Bohac P, Sasaki K, Gauckler L (1993) J Eur Ceram Soc 12:87
24. Keižonis A, Bogusz W, Krok F, Dygas J, Orliukas A, Abrahams I, Gebicki W (1999) Solid State Ionics 119:145